Near Earth Asteroid Rendezvous (NEAR) Navigation Using Altimeter Range Observations

J. J. Bordi,[1] J. K. Miller,[1] B. G. Williams,[1] and F. J. Pelletier[2]

The Near Earth Asteroid Rendezvous (NEAR) spacecraft is currently in orbit phase around the asteroid Eros. Altimeter range measurements from the laser altimeter instrument onboard NEAR are processed in combination with the primary tracking data types, including Deep Space Network (DSN) tracking and optical landmark tracking. As a backup observation type, the altimeter range measurements are not used to generate the operational orbits. Analysis of the impact of the altimeter observations on the estimation of the Eros shape model and the NEAR orbits is performed. The analysis includes an assessment of the impact of altimeter observations on solution convergence when different combinations of tracking data are used. The effectiveness of using the altimeter observations to estimate the shape model while holding the orbits fixed is examined, and, similarly, the effect of estimating the orbits while holding the shape model fixed is examined.

I. Introduction

The Near Earth Asteroid Rendezvous (NEAR) spacecraft was inserted into orbit around the asteroid Eros on February 14, 2000. A complete overview of the NEAR spacecraft and mission design is provided in [1] and [2]. As the first spacecraft to orbit a small body, it has provided many unique challenges and opportunities in the area of spacecraft navigation. One area of investigation is assessing the value of using altimeter range measurements as a primary observation type in spacecraft navigation. The NEAR laser range (NLR) instrument onboard NEAR supplies the altimeter range measurements. However, the NLR observations are not used as one of the primary tracking types in producing the operational NEAR ephemerides. The primary tracking types include Deep Space Network (DSN) radio metric Doppler and range observations as well as optical landmark tracking. The purpose of this study is to see if the addition of altimeter range data in the orbit determination procedure can improve not only the orbits but also the estimates of the central body's physical parameters. Using these results, the future impact of altimeter range data on navigation systems for new missions to small bodies may be assessed, including both ground-based and onboard implementations.

---

[1] Navigation and Mission Design Section.

[2] Center for Space Research, The University of Texas at Austin.

The research described in this publication was carried out by the Jet Propulsion Laboratory, California Institute of Technology, under a contract with the National Aeronautics and Space Administration.

The altimeter provides a measure of the distance from the spacecraft to the point on the surface of the body being illuminated. An advantage of the altimeter data is that the measurements can be taken continuously, without the sunlight restrictions of optical landmark tracking or the station visibility restrictions of DSN tracking. On the other hand, the altimeter range measurements are weakened by the fact that they are made relative to the surface, which is an unknown height above the body's center of mass. Therefore, the shape model usually needs to be estimated simultaneously with the spacecraft's orbit in order to prevent errors in the surface model from being aliased into the orbits. The temporal and geographical density of the observations make it feasible to estimate both the shape model and the orbit at the same time, provided that there is a sufficient amount of a complementary data type available (e.g., DSN radio metric or optical tracking data).

The asteroid Eros is shaped irregularly, with the principal semi-axes measuring roughly 16.5, 8.0, and 6.5 km. For a description of Eros, see [3], which provides the current best estimates of the Eros physical parameters. After orbit insertion, NEAR orbited Eros at relatively high altitudes ranging from 500 to 200 km. This made the initial orbit phase not very useful for assessing the performance of the NLR instrument on spacecraft navigation, since the instrument was designed to be most effective at a range of 50 km. Additionally, during this time frame, NEAR was orbiting Eros at fairly low inclinations. This meant that large areas of the asteroid were not covered by altimeter observations. This is important since, in order to get a good estimate of the Eros shape model, a good geographical distribution of altimeter measurements is needed. For these reasons, this study concentrates on the orbit phase beginning on April 2, 2000. This date coincides with the maneuver that put NEAR in a 200×100 km transfer orbit with an inclination of 57 deg. On April 11, NEAR was inserted into a near-circular 100-km orbit with an inclination of 59 deg. Then, on April 22, NEAR was placed in a 100×50 km transfer orbit, with an inclination of 64 deg. This orbit was maintained until April 30, when the spacecraft was inserted into a near-circular 50-km polar orbit. Obviously, the circular 50-km polar orbit provides the best opportunity for assessing the impact of the NLR observations, since the altitude is within the instrument design range and the polar orbit provides global coverage of Eros. For more detailed information on the NEAR orbital plan, see [4].

II. The Reference Orbits

The NEAR operational orbits are used as reference orbits in this study. These orbits are computed using both the DSN and optical landmark tracking data. These reference orbits are used for comparison purposes in an effort to provide a benchmark for the orbits computed using the NLR data. When the reference orbits are computed, the parameters outlined in Table 1 are estimated. This table also includes the a priori uncertainties assigned to each of these parameters.

The reference orbits are computed with the observation data weighted as follows: the Doppler data are assigned an uncertainty of 0.0056 Hz, the radio metric range observations are weighted with an uncertainty of 100 m, and the optical landmark tracking is processed with an a priori uncertainty of 1 pixel. For a data arc spanning April 2 through June 16, the rms of the 68,880 Doppler residuals is 0.0031 Hz, the rms of the 17,249 radio metric range residuals is 133 m, and the rms of the 2,034 optical residuals is 1.51 pixels. The reference orbits are assumed to be accurate to about the 20-m level. This assumption is based on the data residuals, a posteriori formal uncertainties, consistency of the solutions, and analysis of the estimated physical parameters.

III. Processing the Altimeter Observations

The orbit determination software used in this study (PCODP3)[3] is the operational navigation software used for the NEAR mission and has been written to process DSN radio metric, optical, and altimeter

[3] J. Miller, Jet Propulsion Laboratory, Pasadena, California, 1998.

Table 1. A priori uncertainties for estimated parameters.

Parameter	Uncertainty
Spacecraft position	100 km
Spacecraft velocity	20 mm/s
Asteroid position	60 km
Asteroid velocity	20 mm/s
Asteroid orientation:	
Prime meridian	10 deg
Spin-axis angles	1 deg
Asteroid orientation rate	0.02 deg/s
Stochastic accelerations (1 hour)	0.5 nm/s^2
Solar pressure:	
Gamma	0.01
Beta	0.01
Effective thermal emissivity of spacecraft	0.1%
Maneuver errors	5 mm/s
Landmark locations	700 m
Normalized gravity harmonics (8 × 8)	0.1–0.04

measurements. The formulation used to process the altimeter range measurements is outlined in [5]. To try to account for systematic errors in the altimeter range observations, several kinematic parameters can be estimated. These parameters include a standard range bias. Additionally, a factor is estimated that is intended to account for any performance degradation that may occur in the NLR instrument as the range from the instrument to the illuminated surface point increases. This parameter is based on the fact that the NLR signal weakens an amount proportional to the square of the range. This results in the two-way signal being weakened by an amount proportional to the range to the fourth power. These parameters are then added to the computed observation as follows:

$$R_{\mathrm{alt}} = \left\| \vec{R}_{\mathrm{s/c}} - \vec{R}_{\mathrm{sur}} \right\| + R_{\mathrm{bias}} + F_{\mathrm{degr}} \cdot \left(\left\| \vec{R}_{\mathrm{s/c}} - \vec{R}_{\mathrm{sur}} \right\| \right)^4 + \varepsilon \tag{1}$$

In the equation, $\vec{R}_{\mathrm{s/c}}$ is the position of the spacecraft relative to the center of mass, $\vec{R}_{\mathrm{sur}}$ is the position of the point on the surface of the central body that is illuminated by the altimeter, and ε is the Gaussian noise in the observation. The estimated parameters are the range bias, R_{bias}, and the degradation factor, F_{degr}.

A pointing offset can also be estimated. This parameter is intended to account for a slight misalignment of the NLR instrument that would result in a pointing error with respect to the predefined spacecraft-fixed instrument pointing direction. One cause for such a misalignment could be heat buildup in the spacecraft bus, resulting in flexure of the panels to which the NLR instrument is mounted. The partial of these pointing offsets with respect to the spacecraft position is calculated as follows:

$$
\begin{aligned}
\frac{\partial R_{\text{alt}}}{\partial att_x} &= \left(T_{\text{inert}}^{\text{s/c}} \frac{\partial R_{\text{alt}}}{\partial \vec{R}_{\text{s/c}}} \right)_{x_{\text{s/c}}} \cdot \frac{\partial x_{\text{s/c}}}{\partial att_x} \\
&\simeq \left(T_{\text{inert}}^{\text{s/c}} \frac{\partial R_{\text{alt}}}{\partial \vec{R}_{s/c}} \right)_{x_{\text{s/c}}} \cdot R_{\text{alt}} \\
&= \left[T_{\text{inert}}^{\text{s/c}} \frac{\partial R_{\text{alt}}}{\partial r_{\text{shape}}} \left(\frac{\partial r_{\text{shape}}}{\partial x_{\text{inert}}} \hat{i} + \frac{\partial r_{\text{shape}}}{\partial y_{\text{inert}}} \hat{j} + \frac{\partial r_{\text{shape}}}{\partial z_{\text{inert}}} \hat{k} \right) \right]_{x_{\text{s/c}}} \cdot R_{\text{alt}} \qquad (2)
\end{aligned}
$$

In this equation, $T_{\text{inert}}^{\text{s/c}}$ is a transformation matrix from inertial coordinates to spacecraft-fixed coordinates, att_x is the attitude offset in the spacecraft-fixed x-direction, and r_{shape} is the radius of the shape model. In Eq. (2), the spacecraft-fixed coordinate frame is orientated with the z-direction pointing in the direction that the instruments are pointed. Meanwhile, the xy-plane is aligned with the coordinate frame defined by the line and pixel directions of the optical camera. An equation similar to Eq. (2) is written for the partial with respect to the y-direction pointing offset, as well.

To date, when the NLR instrument is activated, the altimeter measurements are generally made once or twice per second. This results in an immense amount of data, which increases the run time of the orbit determination software significantly. To overcome this, the NLR data are decimated to a 5- or 10-second minimum time interval between sequential observations. This still provides an adequate density of coverage, while making the processing time more reasonable. Figure 1 shows the ground track of the NLR data sampled at a rate of once per 10 seconds, resulting in over 200,000 NLR observations. The ground track plot appears to be much more random or jumbled than typical; there are a few reasons for this. First, over this time span the spacecraft is in several different orbits, with varying inclinations, eccentricities, and altitudes. Second, NEAR, unlike most other altimeter satellites, does not continuously point in the nadir direction. The attitude is constantly changing in order to point the onboard camera and other instruments in the desired direction. Since the NLR instrument is fixed to point in the same direction as the other instruments, the incident angles of the altimeter range measurements are continuously changing as well. Third, the ground track plot is not close to being an equal area map because Eros is so distinctly non-spherical. This results in the appearance of having denser coverage at the long ends of Eros (centered around 0-deg and 180-deg longitude) and more sparse coverage at the shorter radius areas. To illustrate this, Fig. 2 shows four different views of the altimeter coverage on Eros, using the same NLR data collected from April 2 through June 16. In this figure, the black points indicate areas that are covered by NLR observations, while the white areas are portions of the surface that have not been covered by the altimeter ground track. As shown, this time span provides substantial coverage of the asteroid, which is important for estimating the Eros shape model.

IV. Estimating the Shape Model

The Eros shape model is described using spherical harmonic coefficients. To make an estimate of the shape model using the altimeter observations, the operational orbits are used as a reference and are held fixed. This approach ensures that there is no aliasing between the shape model coefficients and the orbits. The only parameters that are estimated are the shape model coefficients, through degree and order 34, the NLR instrument pointing offsets, the NLR range bias, and the NLR altitude degradation factor. All of the parameters are given virtually no a priori constraints, so they are free to adjust. Additionally, NLR points are edited from the solution if the residuals are greater than 600 m. The data arc used spans from April 2 through June 16, which includes 47 days of the circular 50-km polar orbit phase. The NLR data

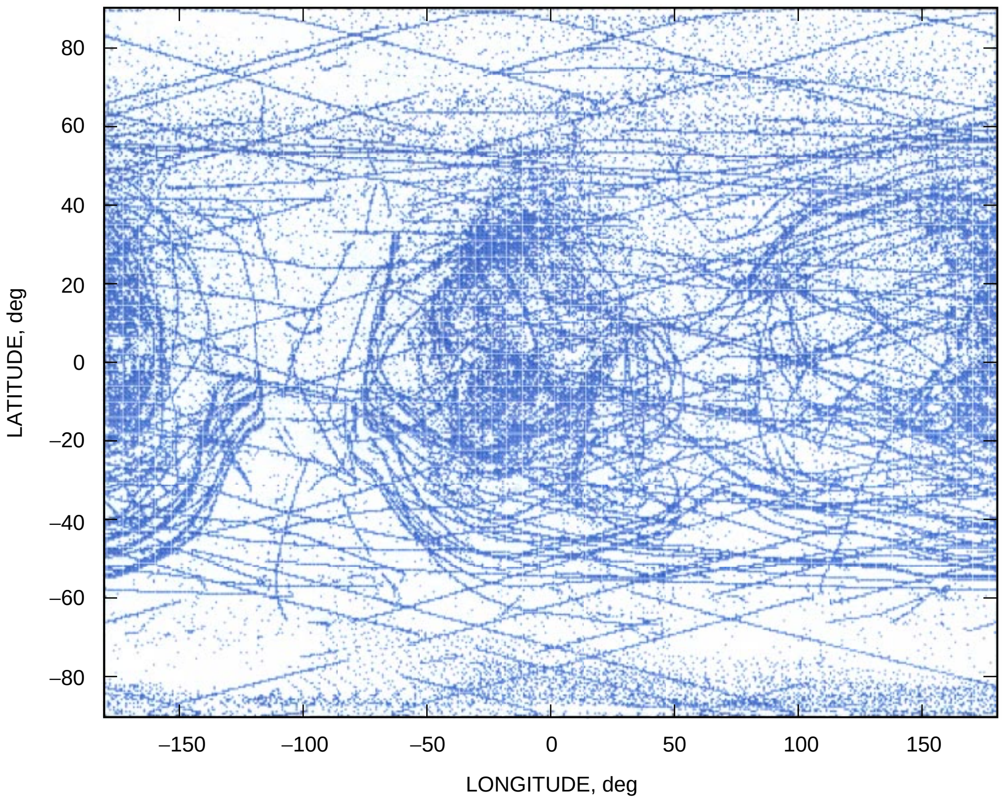

Fig. 1. The NLR ground track from April 2 through June 16, 2000 (10-second sampling, 207,328 observations).

are sampled at a rate of one observation every 5 seconds, resulting in 414,655 measurements. The rms of the NLR residuals is 97 m.

Two aspects are helping provide the separation between the surface harmonics and the pointing errors. First, the orbit altitude and inclination are changing during the orbit arc. This helps by changing the geometry of the NLR observations relative to the same surface points, making constant pointing errors distinguishable from errors in the surface model. Similarly, the changing attitude of the spacecraft results in different observation geometry from pass to pass over the same surface points. This non-nadir pointing of the NLR instrument is also what provides separation between the range bias and the scale of the shape model.

Views of the southern and northern halves of the resulting Eros shape model are shown in Figs. 3 and 4, respectively. The inherent weakness of using spherical harmonics to describe the Eros shape becomes apparent when examining these plots. Since the body is so non-spherical, the spherical harmonics provide a certain amount of resolution near the middle of the asteroid, where the radius is fairly small. However, at the long ends of the asteroid, where the radius is larger, the amount of resolution decreases significantly. This is displayed in the figures, where there are many craters and other surface features visible in the middle of the asteroid, but the surface appears artificially smooth near the long ends. By increasing the degree and order of the estimated harmonics, the level of resolution at the long ends of the asteroid can be increased. However, recent attempts to estimate a shape model through degree and order 50 have not been successful. The resulting shape models appear to break down in the smaller radius areas of the asteroid. It remains to be seen whether including more NLR data corrects this problem.

The value of the estimated pointing error is also of interest. The pointing error of the optical camera has been independently determined to be -1.697 mrad in the x-direction and -0.786 mrad in the

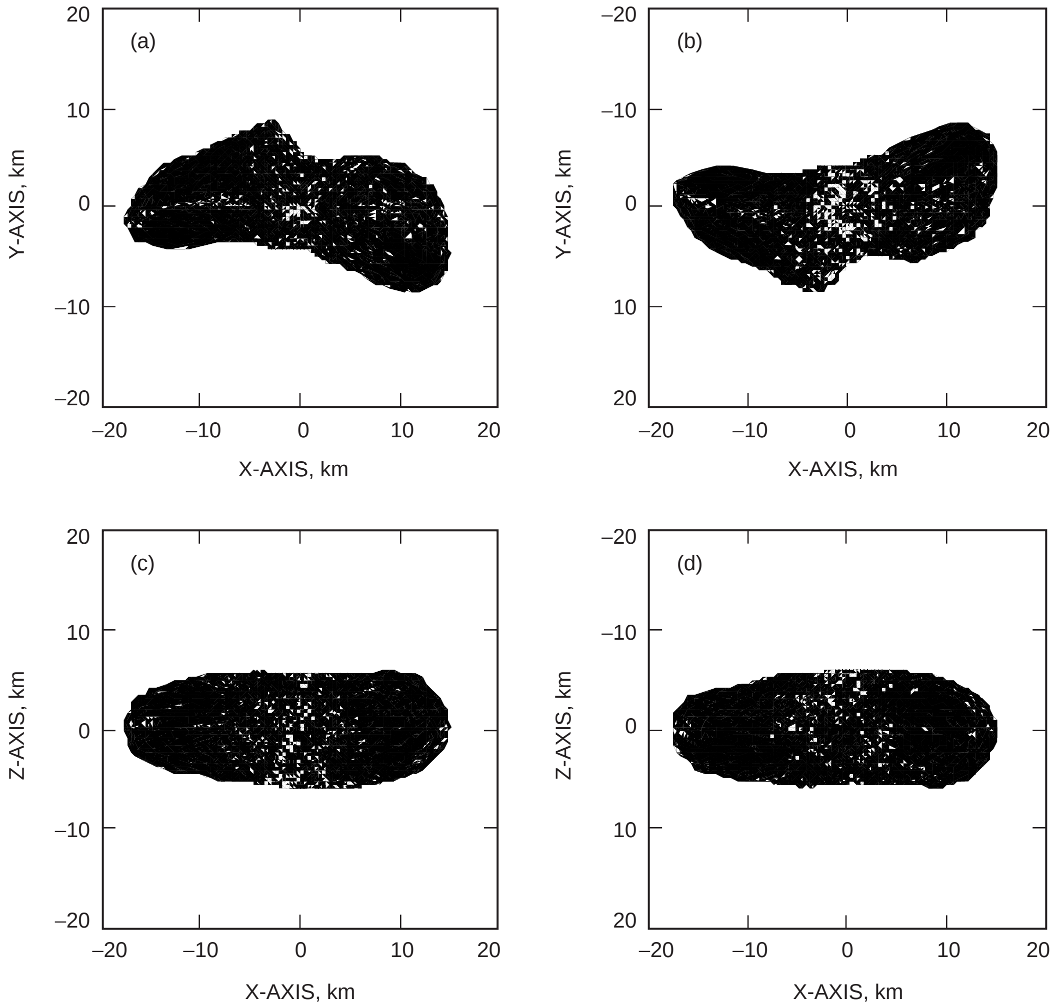

Fig. 2. Four views of the NLR ground track from April 2 through June 16, 2000 (black areas indicate NLR observations and white areas no coverage): (a) northern pole view, (b) southern pole view, (c) negative y-axis view, and (d) positive y-axis view.

y-direction. In this spacecraft-fixed instrument-pointing coordinate frame, the z-axis points in the direction that the scientific instruments are designed to point. The estimated values for the NLR offset are close to the aforementioned values determined for the camera offset, at -1.73 mrad and -0.70 mrad, respectively. This is important since it seems possible that both the camera and NLR instruments could be offset a similar amount, since they are mounted close to each other on the spacecraft. This adds a little more credibility to the values of the estimated offset angles.

The estimate of the range bias is -11.0 m, and the altitude degradation factor is -3.69×10^{-11}. Intuitively, we expect that the degradation factor should be a negative number. This is because, as the distance from the asteroid increases, the weakening of the return NLR signal would make the measurement longer than the true range since the instrument would not sense the return signal until later. These combined estimates equate to an NLR bias of -59 m at a range of 190 km, which is typical of the spacecraft range early in the orbit arc. When the spacecraft is in the 50-km circular orbit, later in the orbit arc, these estimates result in an NLR bias of -11.1 m at a range of 40 km.

In order to show the impact of estimating the NLR-dependent parameters (the pointing offset, range bias, and degradation factor), two shape models complete through degree and order 20 are estimated, one

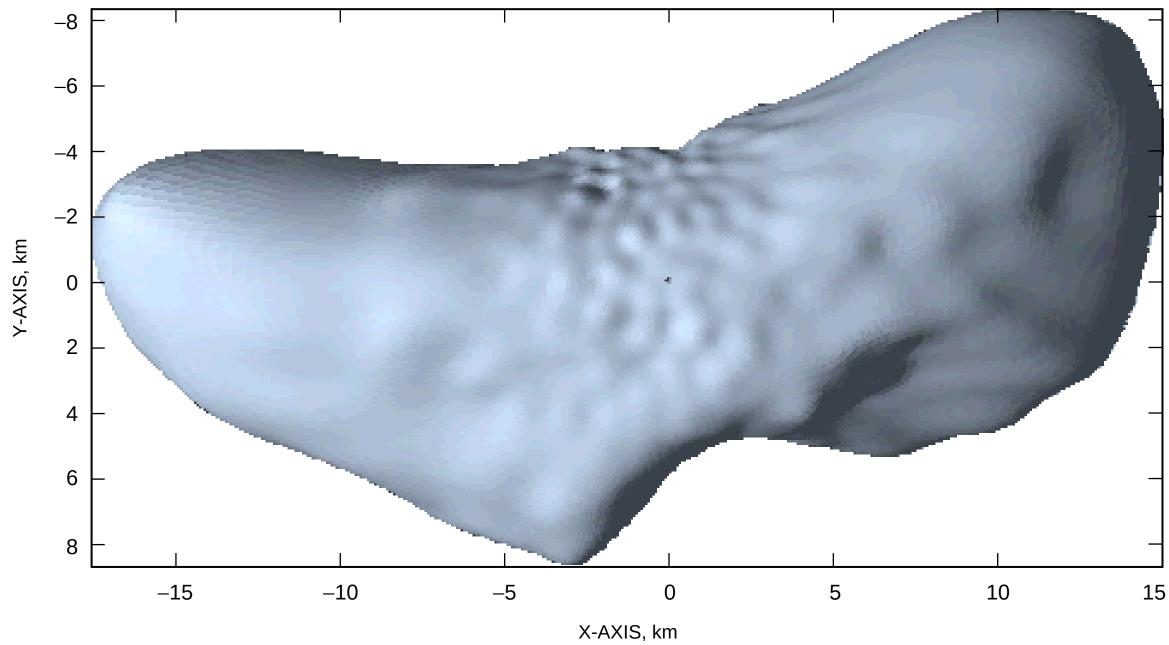

Fig. 3. Southern view of Eros (34 × 34 shape model).

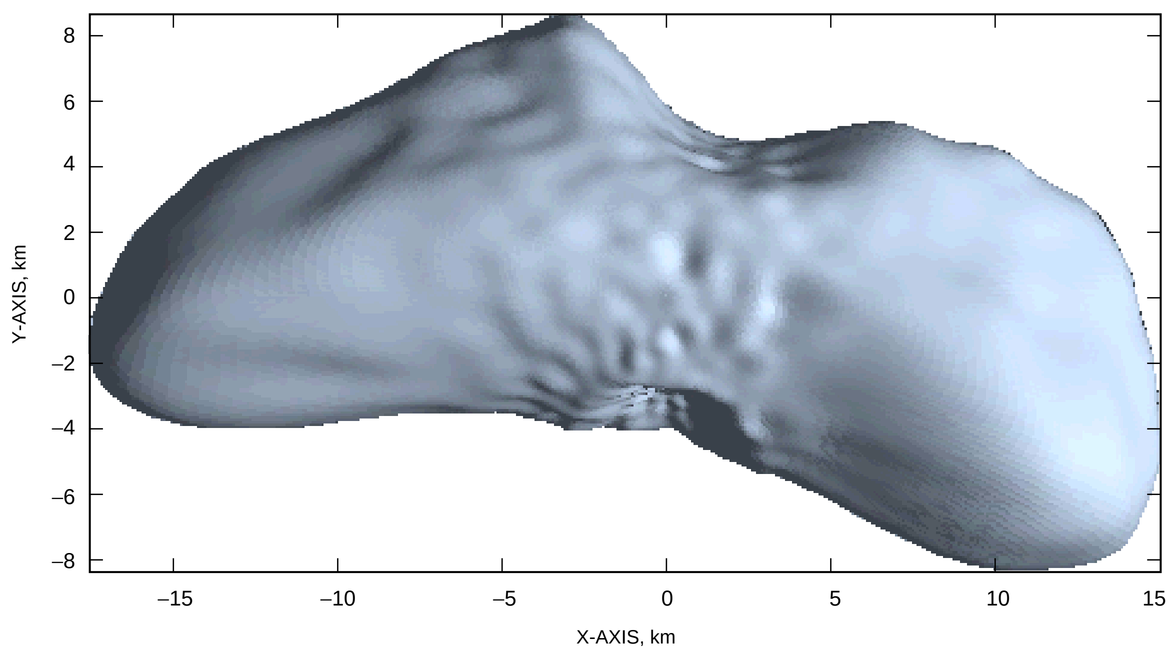

Fig. 4. Northern view of Eros (34 × 34 shape model).

with and one without estimating these parameters. The two shape models are compared by computing the differences at 2-deg intervals in latitude and longitude. The differences between the two shape models are not too large, with the mean of the differences being 28 m and the rms about the mean equal to 82 m.

To show which of these shape models is more accurate, the solutions for the landmark locations are used. These landmark locations are obtained from processing the optical navigation data during the reference orbit solution. The radius of the shape models is calculated at the latitude and longitude of each landmark and compared with the height of the landmark solution. In this comparison, only the 147 best-determined landmarks are used. The results of this comparison are shown in Table 2. It appears that the shape model is more accurate when the NLR-dependent parameters are accounted for in processing the NLR data, as indicated by the reduction in the rms of the differences from 144 to 113 m. Also shown in the table, the rms of the differences between the heights of the landmark solutions and the 34-by-34 shape model is improved further to 73 m.

Since the landmarks are referenced to craters, the actual reference point can often be located above the surface of Eros. This happens because the reference point is chosen as the center of the ellipse that represents the lip of the crater. The center of this ellipse is then above the floor of the crater. This means that we should expect the mean difference between the height of the landmarks and the shape models, evaluated at the landmark locations, to be positive. This turns out to be the case, as is shown in Table 2.

Table 2. Landmark solution heights minus shape model radius.

Shape model	Mean, m	RMS about mean, m
Pointing error unaccounted for (20×20 shape model)	54	144
Pointing errors estimated (20×20 shape model)	26	113
Pointing errors estimated (34×34 shape model)	24	73

V. Computing Orbits while Holding the Shape Model Fixed

In this section, the altimeter data are used to help converge the orbits while holding the shape model estimated in the previous section fixed. The accuracy of the orbits computed in this manner will depend on the accuracy of the reference shape model, since errors in the shape model could be aliased into the orbits. To try to quantify the strength of the altimeter observations in orbit determination, the orbits are computed without the optical landmark tracking. These orbits can then be compared to the reference orbits in order to determine the characteristics of the orbits computed with both radio metric and NLR data. Although the two sets of orbits are not completely independent since both sets contain the radio metric tracking data, the comparison will still give an indication of the impact that the NLR data have on the orbits. The comparison also provides a means to determine the most effective method of processing the NLR data.

The orbit arc used for this comparison starts on May 1 and goes through May 10, which means the orbits occur during the circular 50-km polar orbit phase. The same parameters and a priori uncertainties given in Table 1 are used, with the exception of the landmark positions, which cannot be estimated without using the optical data. The radio metric data are also given the same relative weighting as in the reference orbits, while the NLR data are given an uncertainty of 400 m. The NLR observations are sampled every 30 seconds and are edited when the residuals are greater than 600 m.

The NLR and DSN orbits are computed in three different ways. In case 1, the orbits are computed without estimating or accounting for any of the NLR parameters outlined in Eq. (1) or (2). In case 2, the orbits are computed while applying the pointing error that was obtained during the shape model solution, but without including either the range bias or the degradation factor. In case 3, the pointing error, the range bias, and the degradation factor, as determined in the shape model solution, are all applied. Additionally, the range bias is allowed to adjust minimally; the a priori uncertainty given to the range bias is 10 m.

The three cases are each compared to the reference orbits by differencing each particular test case with the reference orbits every 2 minutes in the Radial, Transverse (along-track), and Normal (RTN) directions. Plots and statistics of the differences between the reference orbits and the test case orbits are given in Fig. 5. These comparisons do not provide information on the absolute accuracy of the orbits, since both sets of orbits contain the same DSN tracking data. However, this test does indicate that the orbits computed with the NLR data seem to be more accurate when the NLR parameters are accounted for. From the figure, it is apparent that better agreement with the reference orbits is achieved during each successive test case. For instance, when the pointing error is accounted for (in going from case 1 to case 2), the orbits show a significant improvement in the transverse direction. Likewise, when the range bias and degradation factor are accounted for, there is a significant improvement in the radial direction (in going from case 2 to case 3). Improvement in the normal direction is also observed in each successive test case.

However, even in case 3, a 40-m transverse bias remains in the NLR orbits. This biasing indicates that there might be an additional error source in the NLR data, which is not accounted for properly. Besides an additional pointing error, this could also be due to a time-tag error on the NLR observation records. Another possible source of error could be changes in performance of the NLR instrument as the incident angle with respect to the illuminated surface changes. At the present time, effective methods of determining either of these possible quantities have not been explored.

VI. Computing the Orbits with only NLR Data

In this section, the orbits are computed without the direct contribution of the radio metric tracking data. This is of interest for autonomous navigation of spacecraft orbiting small bodies. However, these orbits will still have an indirect link to both the radio metric and optical landmark tracking. This indirect contribution is due to the fact that the shape model used was estimated from the reference orbits, which were computed with both the radio metric and optical tracking data.

The same parameters and a priori uncertainties are used as in the last section, except that the gravity harmonics are no longer estimated. The NLR-dependent parameters are also held fixed to the estimates obtained in the long-arc shape model solution. For the 10-day orbit arc, the rms of the NLR residuals is 108 m. Figure 6 shows the RTN differences and statistics between this orbit and the reference orbit. By assuming that the orbit differences are completely due to the NLR-only orbit errors, this comparison indicates that the accuracy of the NLR-only orbits is on the order of 100 m, in a three-dimensional sense.

VII. Orbit Arc Endpoint Comparisons

To determine an estimate of the absolute accuracy of the orbits, comparisons of orbit arc endpoints can be made. In this test, 11 adjacent 5-day orbit arcs are processed. Since there is no overlap between the adjacent arcs, there are no common tracking data used in the two solutions, which keeps the results conservative. The rms of the 10 differences between the orbit endpoints is shown in Table 3 for orbits computed using three different combinations of the tracking data. The first case is the reference case, where the orbits are computed using the radio metric and optical tracking data. From the table, the accuracy of these orbits is about 20 m in a three-dimensional sense. The second case is where the NLR data are substituted for the optical tracking data. This test indicates that the quality of the orbits suffers in all three directions, with the three-dimensional orbit accuracy approaching 40 m. The last case is for the orbits computed using just the NLR data. This results in a large increase in the amount of orbit error in the transverse direction, resulting in a three-dimensional orbit accuracy of approximately 85 m.

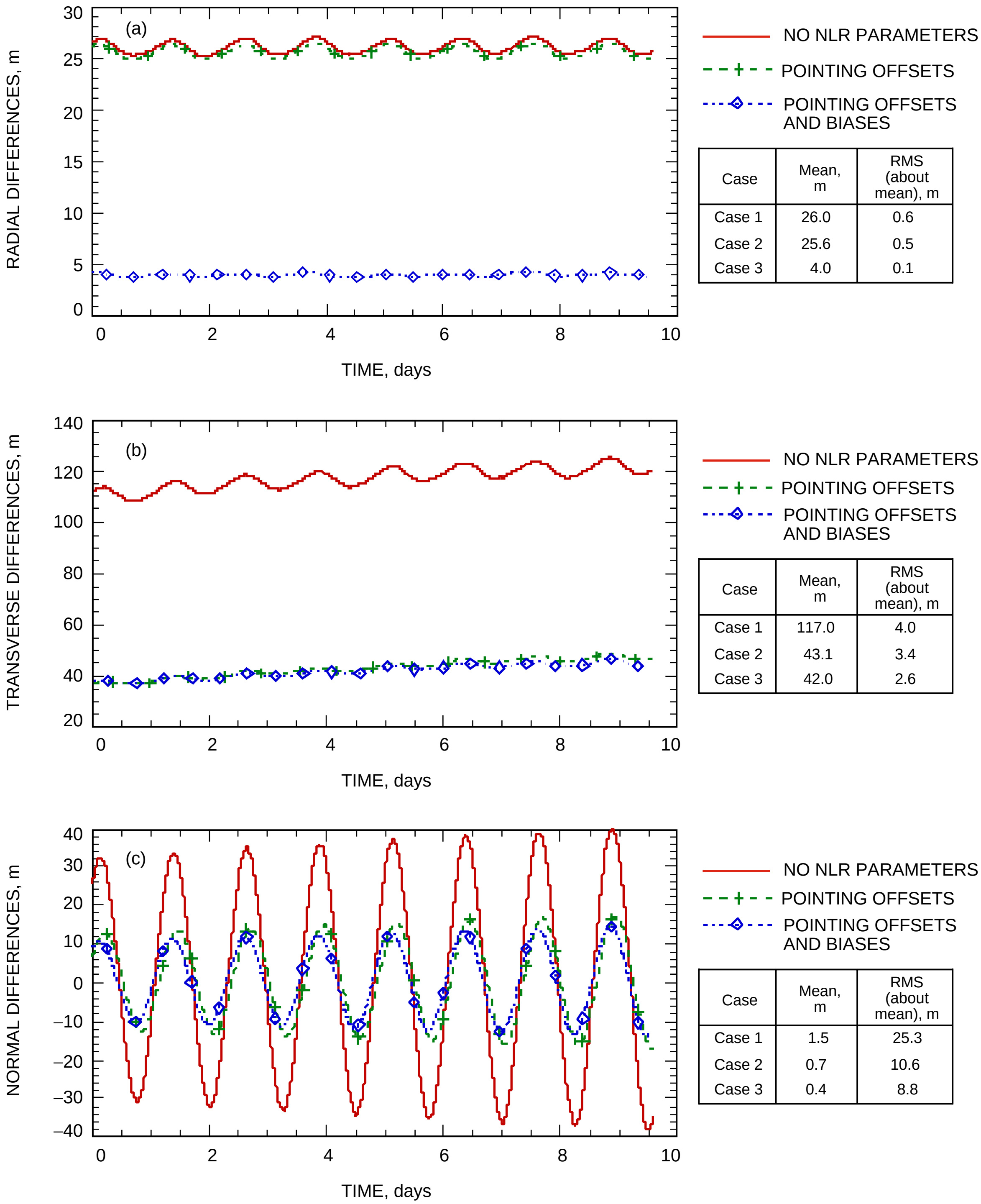

(a)

Case	Mean, m	RMS (about mean), m
Case 1	26.0	0.6
Case 2	25.6	0.5
Case 3	4.0	0.1

(b)

Case	Mean, m	RMS (about mean), m
Case 1	117.0	4.0
Case 2	43.1	3.4
Case 3	42.0	2.6

(c)

Case	Mean, m	RMS (about mean), m
Case 1	1.5	25.3
Case 2	0.7	10.6
Case 3	0.4	8.8

Fig. 5. RTN differences between orbits computed with LIDAR versus orbits computed with optical navigation (DSN used in both cases): (a) radial direction, (b) transverse direction, and (c) normal direction.

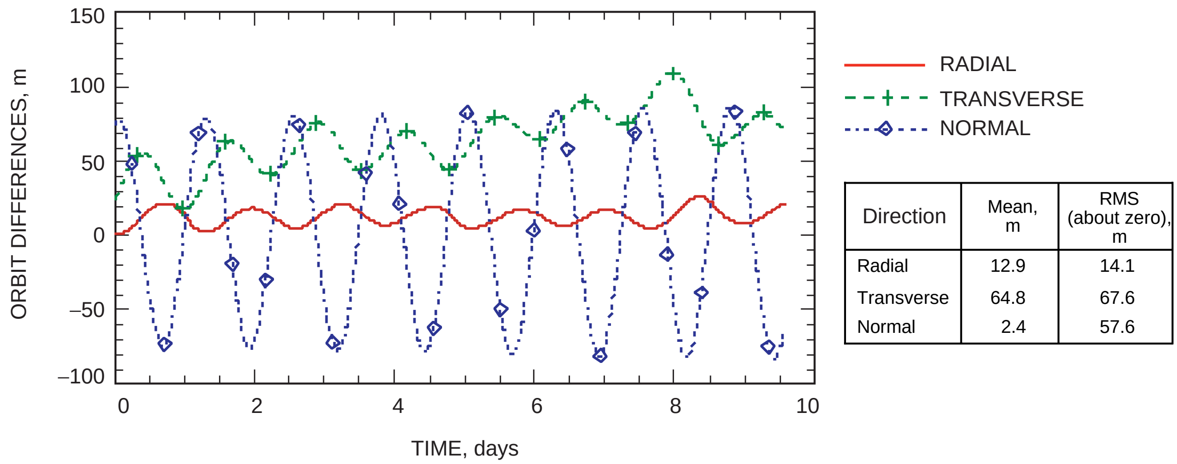

Fig. 6. RTN differences between orbits computed with only NLR tracking versus orbits computed with DSN and optical navigation tracking.

Table 3. RMS of differences between 11 orbit arcs.

Direction	Radio metric and optical tracking, m	Radio metric and NLR tracking, m	NLR tracking alone, m
Radial	13.1	28.0	15.6
Transverse	14.1	24.1	77.8
Normal	3.1	9.6	32.5
Three-dimensional	19.5	38.1	85.7

VIII. Crossover Considerations

In order to improve the impact of NLR data on spacecraft navigation, the concept of crossovers can be introduced to assess the accuracy of an orbit and to possibly reach a better estimate.

Crossover points are defined when the altimeter ground track intersects itself on the surface of the orbiting body. The difference in two satellite altimeter ranges interpolated at a crossover point along their respective ground tracks can thus form a new set of data. In theory, these crossover measurements should bear zero values since the ground track location is the same in both cases. However, errors in the estimate associated with the model will produce residuals that can be minimized to improve some parameters, such as the orbit state.

For NEAR, each NLR measurement includes a pointing direction, which is used to determine the illumination point of the observation on the Eros surface (latitude and longitude). Determination of a crossover point will utilize the following technique, as described in [6].

Let $r_1(t_1)$ and $r_2(t_2)$ be two ground track trajectory vectors referenced to the Eros body fixed frame, where t_1 and t_2 are time tags used as independent variables of the two trajectories. The ground track crossing condition for the two trajectories can be simply written as

$$\hat{r}_1(t_1) = \hat{r}_2(t_2) \tag{3}$$

where $\hat{r}_1$ and $\hat{r}_2$ are Eros-centered unit vectors pointing in the direction of r_1 and r_2, respectively. Let F denote the direction cosine between $\hat{r}_1$and $\hat{r}_2$, i.e.:

$$F(t_1, t_2) = \hat{r}_1(t_1) \cdot \hat{r}_2(t_2) \tag{4}$$

Locating ground track crossovers can be considered a two-dimensional root-finding problem of a single scalar equation,

$$F(t_1, t_2) = 1 \tag{5}$$

which replaces the vector condition in Eq. (3). Since F yields its maximum value of 1 at a crossover, the problem can be solved by using the following condition:

$$\left.\begin{aligned} \frac{\partial F}{\partial t_1} &= \dot{\hat{r}}_1 \cdot \hat{r}_2 = 0 \\ \frac{\partial F}{\partial t_2} &= \hat{r}_1 \cdot \dot{\hat{r}}_2 = 0 \end{aligned}\right\} \tag{6}$$

Given a point $\{t_1, t_2\}$ close to a crossover solution, the Newton–Raphson iteration scheme,

$$\begin{Bmatrix} t_1 \\ t_2 \end{Bmatrix}_{n+1} = \begin{Bmatrix} t_1 \\ t_2 \end{Bmatrix}_n - \begin{bmatrix} \ddot{\hat{r}}_1 \cdot \hat{r}_2 & \dot{\hat{r}}_1 \cdot \dot{\hat{r}}_2 \\ \dot{\hat{r}}_1 \cdot \dot{\hat{r}}_2 & \hat{r}_1 \cdot \ddot{\hat{r}}_2 \end{bmatrix}_n^{-1} \begin{Bmatrix} \dot{\hat{r}}_1 \cdot \hat{r}_2 \\ \hat{r}_1 \cdot \dot{\hat{r}}_2 \end{Bmatrix}_n \tag{7}$$

may converge to a solution. Furthermore, a converged solution will yield a crossover when Eq. (3) is satisfied.

The associated crossover measurement is the difference between the respective ground track trajectory vectors r_1 and r_2, interpolated at t_1 and t_2, respectively. Information on the magnitude of r_1 and r_2 can be obtained using either the shape model or a combination of the spacecraft trajectory and NLR measurement. This technique is currently under testing and results have yet to be determined.

IX. Summary

This study has attempted to quantify the impact of adding altimeter range observations into the orbit determination problem when a spacecraft is orbiting a small body. The analysis was done using altimeter range data from the NEAR spacecraft, which is currently orbiting the asteroid Eros. By holding the orbits computed with radio metric and optical data fixed, the altimeter range data are successfully used to estimate an Eros shape model. Also, during this process estimates for the NLR pointing error, range bias, and altitude degradation factor were obtained. The value for this pointing error is close to the independently observed pointing error for the camera, making the estimate more credible. The shape model also agrees at the sub-100-m level with the landmark heights, which are determined through the optical tracking data.

The orbits computed with the NLR data and the radio metric data together agree with the operational orbits at about the 40- to 50-m level. Even after estimating a pointing error, range bias, and degradation factor, the NLR data seem to bias the orbits, especially in the transverse direction. The complete cause and fix for this biasing have yet to be determined. Likely causes of this could be time-tag errors, instrument performance problems, or additional pointing errors that are not accounted for.

Estimating the orbits using just the NLR data was evaluated. This resulted in a degradation of the accuracy of the orbits to the sub-100-m level. For future missions, this level of accuracy may be acceptable; however, these results were obtained by using the radio metric and optical data to help create the reference shape model.

As the mission progresses, more and more NLR data will be accumulated. These data, especially in the 50-km and 35-km orbits, will allow the processing techniques to be further refined. Hopefully, this will also shed some light on the cause of the biasing of the orbits estimated with the NLR data. Also, adding an algorithm to process altimeter crossovers in the orbit determination software may prove beneficial. This type of measurement would eliminate errors in the shape model from being aliased into the estimated orbits. This may give more strength to the altimeter data and make them a more valuable tool in terms of orbit determination.

Acknowledgment

The authors acknowledge Dr. Yanping Guo of Johns Hopkins University, Applied Physics Laboratory, for supplying the NLR data used in this study.

References

[1] R. W. Farquhar, "Introduction: The Near-Earth Asteroid Rendezvous (NEAR) Mission," *The Journal of the Astronautical Sciences*, vol. 43, no. 4, pp. 349–352, October–December 1995.

[2] R. W. Farquhar, D. W. Dunham, and J. V. McAdams, "NEAR Mission Overview and Trajectory Design," *The Journal of the Astronautical Sciences*, vol. 43, no. 4, pp. 353–372, October–December 1995.

[3] J. K. Miller, P. G. Antreasian, R. W. Gaskell, J. Giorgini, C. E. Helfrich, W. M. Owen, B. G. Williams, and D. K. Yeomans, "Determination of Eros Physical Parameters for Near Earth Asteroid Rendezvous Orbit Phase Navigation," AAS/AIAA Astrodynamics Specialist Conference, Paper AAS99-463, Girdwood, Arkansas, August 16–18, 1999.

[4] C. E. Helfrich, J. K. Miller, P. G. Antreasian, E. Carranza, B. G. Williams, D. W. Dunham, R. W. Farquhar, and J. V. McAdams, "Near Earth Asteroid Rendezvous (NEAR), Revised Eros Phase Trajectory Design," AAS/AIAA Astrodynamics Specialist Conference, Paper AAS99-464, Girdwood, Arkansas, August 16–18, 1999.

[5] J. J. Bordi, P. G. Antreasian, J. K. Miller, and B. G. Williams, "Altimeter Range Processing Analysis for Spacecraft Navigation about Small Bodies," AAS/AIAA Space Flight Mechanics Meeting, Paper AAS00-165, Clearwater, Florida, January 23–26, 2000.

[6] M. C. Kim, "Theory of Satellite Ground Track Crossovers," *Journal of Geodesy*, vol. 71, pp. 749–767, 1997.